Diamagnetic Response of Exciton Complexes in Semiconductor Quantum Dots

Ming-Fu Tsai,[1] Hsuan Lin,[2] Chia-Hsien Lin,[2] Sheng-Di Lin,[1] Sheng-Yun Wang,[2] Ming-Cheng Lo,[1] Shun-Jen Cheng,[2] Ming-Chih Lee,[2] and Wen-Hao Chang[2,*]

[1]*Department of Electronic Engineering, National Chiao Tung University, Hsinchu, 300 Taiwan*
[2]*Department of Electrophysics, National Chiao Tung University, Hsinchu, 300 Taiwan*

(Received 11 June 2008; published 24 December 2008)

We report measurements of diamagnetic shifts for different exciton complexes confined in small InAs quantum dots. The measured diamagnetic responses are sensitive to the number of carriers in the exciton complexes, with systematic differences between neutral excitons, biexcitons, and trions. Theoretical calculations suggest that such systematic differences arise from very different extents of electron and hole wave functions confined in small quantum dots. The measured magnetic response of Coulomb energies is found to vary with the cube of the wave function extent, and can be a sensitive probe to the electron-hole wave function asymmetry.

DOI: 10.1103/PhysRevLett.101.267402 PACS numbers: 78.67.Hc, 78.55.Cr

Excitons confined in semiconductor quantum dots (QDs) have been proven to be well suited for photonics-based quantum information processing, such as single-photon emitters [1] and quantum logic gates [2]. To manipulate the charge and spin of excitons confined in a QD, it is necessary to understand the Coulomb interactions among the constituent charge carriers, as well as their responses to a magnetic field B. For neutral excitons (X), the exciton energy increases quadratically with B, i.e., the diamagnetic shift ($\Delta E = \gamma B^2$) [3–6]. The measured diamagnetic coefficient reflects not only the QD's spatial confinement, but also the interparticle Coulomb interactions, because the magnetic field squeezes the exciton wave function, which in turn enhances the binding energy and hence reduces the overall diamagnetism. This picture is well established, and has long been used to analyze the diamagnetic shifts of X confined in various nanostructures [4–9]. However, the magnetic responses of confined exciton complexes, such as biexcitons (XX) and trions (either X^+ or X^-) consisting of more charged particles than a neutral exciton, are still less well known to date. The behavior of XX and $X^{\pm}$ are potentially much more interesting, because their singlet spin configuration and the lack fine-structure splitting are of great importance for many quantum optics applications, such as the optical preparation of pure spin states [10,11], as well as the generation of entangled photon pairs [12]. Although a few data for the diamagnetic shifts of XX and $X^{\pm}$ have been reported [13–15], a quantitative understanding for the magnetic response of an exciton complexes has yet to be established.

Here, we report systematic measurements of diamagnetic shifts for different exciton complexes strongly confined in small InAs self-assembled QDs. We demonstrate for the first time that the diamagnetic responses are sensitive to the number of carriers in the exciton complexes, with systematic differences between neutral excitons, biexcitons, and trions. Theoretical calculations indicate that such systematic differences could be observed only when the confined electron and hole wave functions exhibit a large difference in their lateral extents. Furthermore, the magnetic response of Coulomb energy was found to scale as the cube of its single-particle wave function extent, and can be a sensitive probe to the electron-hole wave function asymmetry.

The sample (LM4596) was grown by molecular beam epitaxy. A layer of InAs self-assembled QDs (2.0 MLs) was grown on GaAs at 480 °C without substrate rotations, yielding a gradient in dot density on the wafer ranging from 10^8 to 10^{10} cm^{-2}. The QDs were finally capped by a 100-nm undoped GaAs layer. Atomic force microscopy of uncapped samples reveals that the InAs QDs are lens-shaped, with an average height and diameter of $\approx 2 \pm (0.5)$ and ≈ 15 nm, respectively. For embedded dots, the dot sizes are expected to be even smaller. Single dot spectroscopy were performed in a micro-photoluminescence (μ-PL) setup combined with a 6-T superconducting magnet. The PL signals were analyzed by a 0.75-m grating monochromator combined with a liquid-nitrogen-cooled charge-coupled device (CCD) camera.

The Coulomb interactions between electron-electron (e-e), electron-hole (e-h), and hole-hole (h-h) in individual QDs were first investigated by μ-PL measurements. In Fig. 1(a), the PL spectra measured at $T = 8$ K for six different QDs are displayed. In spite of the wide spread in emission energy (1330–1390 meV), the spectral feature is very similar. Four emission lines associated with the recombination of X, XX, X^+ and X^- can be observed. These emission lines have been identified based on power-dependent and polarization-resolved PL measurements. X and XX lines were first identified by their linear and quadratic power dependencies of intensities [see Fig. 1(b)]. The neutral and charged excitons were then distinguished by polarization-resolved measurements. Emissions from X and XX are known to exhibit polarization doublets with

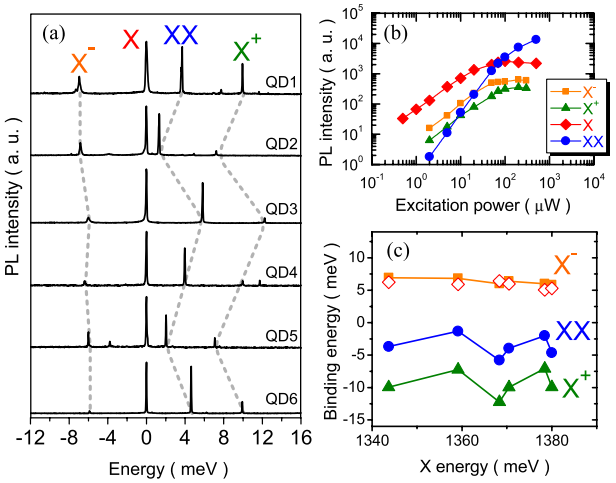

FIG. 1 (color online). (a) PL spectra taken from six different QDs. The energy scale is relative to the X peak energy at 1343.7, 1359.2, 1368.4, 1370.5, 1378.4 and 1380.0 meV from QD1 to QD6, respectively. (b) Power-dependent PL intensity of X, XX, X^+ and X^- for the QD3. (c) Binding energies as a function of the X emission energy. The open symbols are $E^b_{XX} - E^b_{X^+}$ that coincides very well with $E^b_{X^-}$.

the same fine-structure splitting (FSS) due to the e-h exchange interaction [16]. The lack of measurable FSS can thus be used to distinguish X^+ and X^- states from the X state.

The binding energy of XX, X^+ and X^-, with respect to X, are shown in Fig. 1(c). In all cases, the biexciton binding energy $E^b_{XX}(\equiv E_X - E_{XX})$ is negative (i.e., antibinding), varying from -1 to -6 meV for different dots, whereas the X^- binding energy is almost fixed at about $E^b_{X^-} \approx 6.2 \pm 0.4$ meV. Interestingly, the X^+ binding energy $E^b_{X^+}$ also shows a variation similar to that of XX, but with a larger binding energy ranging from -7 to -12 meV. This result highlights the importance of the imbalanced Coulomb repulsions and attractions caused by the different spatial extents of electron (l_e) and hole (l_h) wave functions. The sign of these binding energies indicates that $l_h < l_e$; i.e., the holes are more localized in the QDs. Quantitatively, the direct Coulomb interaction between e-e (V_{ee}), e-h (V_{eh}), and h-h (V_{hh}) can be treated as perturbations to the single-particle state in the strong confinement regime. If the correlation effect is excluded as a first approximation, the binding energy for X^- (X^+) is given by $E^b_{X^-} = V_{eh} - V_{ee}$ ($E^b_{X^+} = V_{eh} - V_{hh}$), while the XX binding energy is given by $E^b_{XX} = 2V_{eh} - V_{hh} - V_{ee}$. Because $l_h < l_e$, a small change in l_h can lead to a large variation in V_{hh}. Therefore, it can be inferred that the variation in the XX and X^+ energies arise mainly from the fluctuation in l_h among different dots. As shown in Fig. 1(c), we can see that $E^b_{XX} - E^b_{X^+} \approx E^b_{X^-}$, as expected for the first-order approximation in the strong confinement regime.

The wave function extents and their responses to the applied magnetic field B were investigated by magneto-PL measurements. A typical result is shown in Fig. 2. The magnetic field was applied along the growth direction (Faraday geometry). In this geometry, each line splits into a doublet by the Zeeman effect. The deduced g factor of X is $g = 3.0 \pm 0.1$ for all investigated QDs, and is identical with that of XX and $X^\pm$ within our detection accuracy. The diamagnetic shifts reveal a quadratic dependence on B, as expected in the weak-field limit. As illustrated in Fig. 2(b), the average energy of each doublet was fitted to γB^2, from which the diamagnetic coefficient γ can be obtained for each exciton complex. Figure 3 displays the diamagnetic coefficients of X and XX for different QDs as a function of the X emission energy. All the investigated QDs show a small exciton diamagnetic coefficient γ_X, ranging from 7 to 11 μeV/T^2, and getting larger with the increasing X energy. These γ_X values are significantly smaller than the bulk value (109 μeV/T^2) and the two-dimensional (2D) quantum limit value (20 μeV/T^2) [6], indicating a strong confinement. In addition, we found that the biexciton diamagnetic coefficient γ_{XX} is $\sim$30($\pm$10)% smaller than γ_X. A nearly identical reduction in γ_{X^+} was also observed, as shown in Fig. 3.

To understand the underlying mechanism of the reduced diamagnetism, theoretical model calculations were performed. Because the QD shape is rather flat, the 3D exciton problem can be reduced to an effective 2D problem by using the adiabatic approximation [8,17]. For simplicity, we take a 2D parabolic potential as the effective lateral confinement for both electrons and holes with a quantization energy of $\hbar\omega_\beta$ and a wave function extent of $l_\beta = \sqrt{\hbar/m^*_\beta\omega_\beta}$, where β denotes e or h and m^*_β are the effective masses. The use of parabolic model simplifies the problem considerably, because of the availability of analytical formula for all Coulomb interactions being parameterized by l_β. The interacting Hamiltonian can thus be constructed using the generalized formulations for the

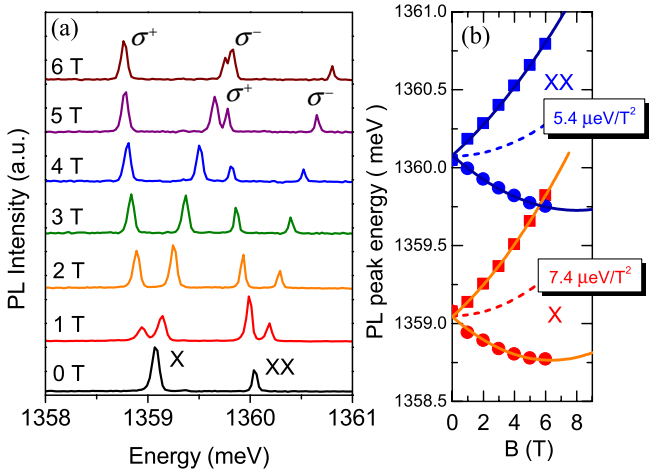

FIG. 2 (color online). (a) Magneto-PL spectra for QD2 measured under $B = 0$–6 T in the Faraday geometry. (b) The B-dependent energy shifts of the X and XX lines. Solid and dashed lines are fitting curves using quadratic B dependence.

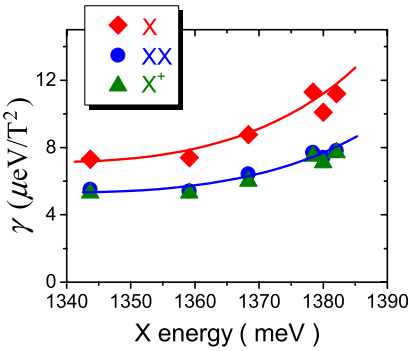

FIG. 3 (color online). Diamagnetic coefficient γ of X, XX, and X^+ for different QDs as a function of the X emission energy.

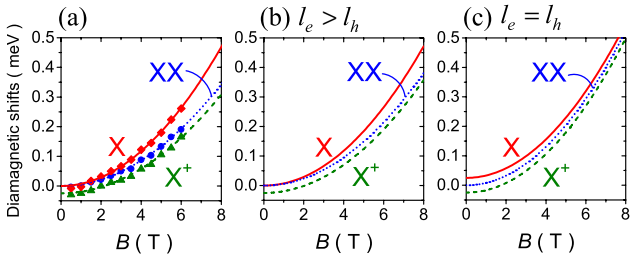

FIG. 4 (color online). (a) Experimental diamagnetic shifts of X, XX and X^+ in QD2. (b) Simulated diamagnetic shifts for different exciton complexes with $l_e = 4.5$ nm and $l_h/l_e = 0.52$. (c) The same as (b) but using $l_e = l_h = 4.5$ nm. The curves for X^+ in all cases and that for X in (c) have been offset by 25 μeV for clarity.

single-particle energy and the Coulomb matrix elements given explicitly in Refs. [18,19]. Predominant Coulomb matrix elements for X, X^-, X^+, and XX states are those involving the lowest s orbital,

$$V_{\alpha\beta} = \frac{e^2}{4\pi\epsilon_0\epsilon_r}\sqrt{\frac{\pi}{2}}\frac{1}{l},$$

where $l \equiv \sqrt{(l_\alpha^2 + l_\beta^2)/2}$ with $\alpha, \beta = e, h$. Because we just focus on the diamagnetic behavior, the Zeeman terms are omitted here for brevity. The energy spectra of neutral and charged exciton complexes were then calculated using the standard configuration-interaction (CI) method within the basis constructed from the low-lying electron and hole shells [18,20].

Using the parameters $l_e = 4.5$–5.6 nm and $l_h/l_e = 0.51$–0.55 with electron (hole) effective mass of $m_e^* = 0.05m_0$ ($m_h^* = 0.5m_0$), we obtained a general agreement with the experimental binding energies and diamagnetic shifts for all investigated dots [20]. The magneto-PL spectra were evaluated by replacing ω_β with the B-dependent hybridized frequencies $\Omega_\beta(B) = \sqrt{\omega_\beta^2 + (\omega_c^\beta/2)^2}$, where $\omega_c^\beta = eB/m_\beta^*$ is the cyclotron frequency. The simulated results of QD2 are plotted in Fig. 4, and compared with experimental diamagnetic shifts. The simulations also predict that the diamagnetic shifts of XX and X^+ are reduced by the same amount from that of X, consistent with our experimental findings [Fig. 4(a)]. From the calculations, we found that the fundamental cause of the reduced diamagnetism is that $l_h < l_e$. In order to highlight this point, simulations using $l_h = l_e$ are also shown in Fig. 4(c), where all exciton complexes show essentially the same diamagnetic shift.

Our calculations make clear how the different l_e and l_h change the overall diamagnetic shifts. The applied magnetic field superimposes a magnetic confinement to the QDs and thereby modifies l_e and l_h accordingly. With the increasing B, the magnetic confinement will be first experienced by the more extended electron wave function. Therefore, the magnetic response of V_{ee} and V_{eh} (Coulomb terms involving electrons) will be more significant than that of V_{hh}. In the weak-field limit, where $\omega_c^\beta \ll \omega^\beta$, the B dependencies of the single-particle energy $\varepsilon_\beta(B)$ and the Coulomb energies $V_{\alpha\beta}(B)$ can be expanded analytically as,

$$\varepsilon_\beta(B) \approx \varepsilon_\beta(0) + \gamma_\beta^{\mathrm{SP}} B^2 + \ldots$$
$$V_{\alpha\beta}(B) \approx V_{\alpha\beta}(0) + \gamma_{\alpha\beta}^{\mathrm{Coul}} B^2 + \ldots$$

where $\gamma_\beta^{\mathrm{SP}} = e^2 l_\beta^2/8m_\beta^*$ is the single-particle diamagnetic coefficient, and $\gamma_{\alpha\beta}^{\mathrm{Coul}} = k(l_\alpha^6 + l_\beta^6)/2l^3$ accounts for the magnetic response of Coulomb energy, with the constant k defined as $(e^2/4\pi\epsilon_0\epsilon_r)(e^2\sqrt{\pi/2}/16\hbar^2)$. If the contributions from the Coulomb term $\gamma_{\alpha\beta}^{\mathrm{Coul}}$ were ignored, i.e., only the single-particle energy is considered, γ_{XX} and γ_{X+} are expected to be the same as $\gamma_X = (\gamma_e^{\mathrm{SP}} + \gamma_h^{\mathrm{SP}}) \approx \gamma_e^{\mathrm{SP}}$, which is dominated by the electron wave function extent and varies as l_e^2. However, the result of $\gamma_X > \gamma_{XX} \simeq \gamma_{X+}$ shown in Fig. 3 indicates that the contributions from Coulomb terms $\gamma_{\alpha\beta}^{\mathrm{Coul}}$ are non-negligible. In fact, one can see that $\gamma_{\alpha\beta}^{\mathrm{Coul}}$ has an even stronger dependence on the wave function extent ($\propto l_\beta^3$). If we take the Coulomb energies as perturbations in the strong confinement regime, the diamagnetic shift of X should be corrected as $\gamma_X = (\gamma_e^{\mathrm{SP}} + \gamma_h^{\mathrm{SP}}) - \gamma_{eh}^{\mathrm{Coul}}$, involving both single-particle and Coulomb contributions. On the other hand, the diamagnetic shift of XX will deviate from that of X by an amount of $\Delta\gamma = \gamma_X - \gamma_{XX} = (2\gamma_{eh}^{\mathrm{Coul}} - \gamma_{ee}^{\mathrm{Coul}} - \gamma_{hh}^{\mathrm{Coul}})$. This accounts for how the different l_e and l_h can lead to very different contributions of the e-e and h-h Coulomb interactions to the overall diamagnetism. Because of $l_h < l_e$ and hence $l_h^3 \ll l_e^3$, we have $\gamma_{ee}^{\mathrm{Coul}} \simeq \gamma_{eh}^{\mathrm{Coul}} \gg \gamma_{hh}^{\mathrm{Coul}}$, that leads to $\gamma_X - \gamma_{XX} = \Delta\gamma \simeq \gamma_{ee}^{\mathrm{Coul}}$. The same arguments can be applied to the X^+ case, where γ_{X+} is also reduced by a similar amount, in agreement with our experimental observations.

Quantitatively, the actual single-particle diamagnetic shift of X can be deduced from $(\gamma_X + \Delta\gamma) \simeq \gamma_e^{\mathrm{SP}} \propto l_e^2$. On the other hand, because $\Delta\gamma \simeq \gamma_{ee}^{\mathrm{Coul}} \propto l_e^3$, a plot of $\Delta\gamma$ vs $(\gamma_X + \Delta\gamma)^{3/2}$ will result in a straight line with a

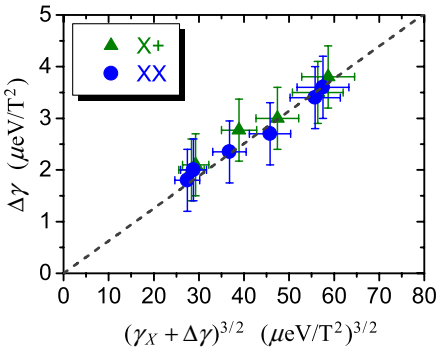

FIG. 5 (color online). A plot of measured $\Delta\gamma$ to $(\gamma_X + \Delta\gamma)^{3/2}$ for both XX and X^+.

slope $\approx k(8m_e^*/e^2)^{3/2}$. Such a plot is shown in Fig. 5, where the experimental data of XX and X^+ for all investigated QDs agree quantitatively with the model prediction. This unambiguously demonstrates that the magnetic response of Coulomb energy $\gamma_{ee}^{\mathrm{Coul}}$ scales as l_e^3. Interestingly, the slope shown in Fig. 5 corresponds to an electron effective mass of $m_e^* = 0.05m_0$. This value is close to but somewhat larger than the theoretical value of strained InAs islands ($0.042m_0$) [21]. It implies that the electron wave function has penetrated into the barrier material ($m_{e,\mathrm{GaAs}}^* = 0.067m_0$), leading to an increased effective mass [8]. This reasoning is also supported by the result shown in Fig. 3, where a systematic increase of diamagnetic shift with the increasing emission energy can be seen. Such an increasing trend implicates that the electron gradually loses confinement as the dot size reduces [8], which will push the electron level toward the wetting-layer continuum, resulting in a more extended electron wave function penetrating into the barrier material. On the other hand, the hole wave function remains well localized in the QDs. This explains why the estimated $l_h/l_e \approx 0.53$ for our QDs is smaller than the reported ratio of $\sim$0.75 for typical In(Ga)As/GaAs self-assembled QDs [15,19].

We would like to emphasize that the systematic differences in diamagnetic shift could be observed only when the confined electron and hole wave functions exhibit a large difference in their lateral extents. Small InAs QDs investigated here just meet this requirement. For larger In(Ga)As QDs, since l_e and l_h are expected to be similar, the diamagnetic response of all exciton complexes will be nearly identical [13,15], so that the magnetic response of interparticle Coulomb energies of such strongly confined few-particle systems becomes unable to resolve experimentally.

In summary, the diamagnetic responses of different exciton complexes confined in small InAs/GaAs QDs have been investigated. Systematic differences between the diamagnetic shifts of neutral excitons, biexcitons, and trions were observed. Our experimental results provide a general guideline of how the interparticle Coulomb interactions affect the overall diamagnetism of such strongly confined few-particle systems. Whenever the diamagnetic shift was determined experimentally, both the contributions from the single-particle energies and interparticle Coulomb energies can be deduced quantitatively. Most importantly, we found that the magnetic response of interparticle Coulomb energy is even more sensitive to the wave function extent (scales as l^3), as compared with the single-particle energies (l^2) and the direct Coulomb energies (l^{-1}). Therefore, the measured magnetic response of Coulomb interactions can thus be a sensitive probe to the asymmetry of the electron and hole wave function extents. The experimental approach and theoretical arguments reported here can also be applied to other QD systems, providing a way to take a closer look at the detailed electronic structures of various quantum confined systems.

This work was supported in part by the program of MOE-ATU and the National Science Council of Taiwan under Grant No. NSC-96-2112-M-009-014. S. J. C. acknowledges support from the National Center Theoretical Science of Taiwan.

*whchang@mail.nctu.edu.tw

[1] P. Michler *et al.*, Science **290**, 2282 (2000); M. Pelton *et al.*, Phys. Rev. Lett. **89**, 233602 (2002); Z. Yuan *et al.*, Science **295**, 102 (2002); W.-H. Chang *et al.*, Phys. Rev. Lett. **96**, 117401 (2006).
[2] X. Li *et al.*, Science **301**, 809 (2003).
[3] S. N. Walck and T. L. Reinecke, Phys. Rev. B **57**, 9088 (1998).
[4] M. Bayer *et al.*, Phys. Rev. B **57**, 6584 (1998).
[5] Y. Nagamune *et al.*, Phys. Rev. Lett. **69**, 2963 (1992).
[6] T. Someya, H. Akiyama, and H. Sakaki, Phys. Rev. Lett. **74**, 3664 (1995).
[7] P. Pereyra and S. E. Ulloa, Phys. Rev. B **61**, 2128 (2000).
[8] K. L. Janssens, F. M. Peeters, and V. A. Schweigert, Phys. Rev. B **63**, 205311 (2001).
[9] V. Mlinar *et al.*, Phys. Rev. B **75**, 205308 (2007).
[10] M. Atature *et al.*, Science **312**, 551 (2006).
[11] X. Xu *et al.*, Phys. Rev. Lett. **99**, 097401 (2007).
[12] R. M. Stevenson *et al.*, Nature (London) **439**, 179 (2006).
[13] C. Schulhauser *et al.*, Phys. Rev. B **66**, 193303 (2002).
[14] R. J. Young *et al.*, Phys. Rev. B **72**, 113305 (2005).
[15] N. I. Cade *et al.*, Phys. Rev. B **73**, 115322 (2006).
[16] M. Bayer *et al.*, Phys. Rev. B **65**, 195315 (2002); A. Högele *et al.*, Phys. Rev. Lett. **93**, 217401 (2004).
[17] In the weak-field limit, the adiabatic 2D approach and the full 3D treatment give practically the same result, see, e.g., Ref. [8] for detail.
[18] S.-J. Cheng, W. Sheng, and P. Hawrylak, Phys. Rev. B **68**, 235330 (2003); S.-J. Cheng *ibid.* **76**, 075329 (2007).
[19] R. J. Warburton *et al.*, Phys. Rev. B **58**, 16221 (1998).
[20] We consider only one bound electron state but two hole shells in our CI calculations, because the XX^+ features can be observed at higher excitation powers, but still without measurable XX^- lines.
[21] C. Pryor, Phys. Rev. B **57**, 7190 (1998).